# Two Homologous ATP-Binding Cassette Transporter Proteins, AtMDR1 and AtPGP1, Regulate Arabidopsis Photomorphogenesis and Root Development by Mediating Polar Auxin Transport[1]

**Rongcheng Lin and Haiyang Wang***

Boyce Thompson Institute for Plant Research, Cornell University, Ithaca, New York 14853

Light and auxin control many aspects of plant growth and development in an overlapping manner. We report here functional characterization of two closely related *ABC* (ATP-binding cassette) transporter genes, *AtMDR1* and *AtPGP1*, in light and auxin responses. We showed that loss-of-function *atmdr1* and *atpgp1* mutants display hypersensitivity to far-red, red, and blue-light inhibition of hypocotyl elongation, reduced chlorophyll and anthocyanin accumulation, and abnormal expression of several light-responsive genes, including *CAB3*, *RBCS*, *CHS*, and *PORA*, under both darkness and far-red light conditions. In addition, we showed that the *atmdr1-100* and *atmdr1-100/atpgp1-100* mutants are defective in multiple aspects of root development, including increased root-growth sensitivity to 1-naphthalene acetic acid (1-NAA), and decreased sensitivity to naphthylphthalamic acid (NPA)-mediated inhibition of root elongation. Consistent with the proposed role of AtMDR1 in basipetal auxin transport, we found that expression of the auxin responsive *DR5*::*GUS* reporter gene in the central elongation zone is significantly reduced in the *atmdr1-100* mutant roots treated with 1-NAA at the root tips, compared to similarly treated wild-type plants. Moreover, *atmdr1-100*, *atpgp1-100*, and their double mutants produced fewer lateral roots, in the presence or absence of 1-NAA or NPA. The *atmdr1-100* and *atmdr1-100/atpgp1-100* mutants also displayed enhanced root gravitropism. Genetic-epistasis analysis revealed that mutations in *phyA* largely suppress the randomized-hypocotyl growth and the short-hypocotyl phenotype of the *atmdr1-100* mutants under far-red light, suggesting that phyA acts downstream of AtMDR1. Together, our results suggest that AtMDR1 and AtPGP1 regulate Arabidopsis (*Arabidopsis thaliana*) photomorphogenesis and multiple aspects of root development by mediating polar auxin transport.

Light is one of the important environmental factors regulating numerous plant developmental programs including seed germination, seedling deetiolation, leaf expansion, stem elongation, phototropism, stomata opening, chloroplast development and movement, and flower initiation (Wang and Deng, 2004). Arabidopsis (*Arabidopsis thaliana*) seedling development has been adapted as a model system to dissect light control of plant development. In the dark, Arabidopsis seedlings undergo skotomorphogenesis (etiolation) with elongated hypocotyls, closed cotyledons, and apical hooks. Light induces photomorphogenesis (deetiolation) by inhibiting hypocotyl elongation and promoting expansion of cotyledons and development of the proplastids into green chloroplasts to prepare for photosynthesis (McNellis and Deng, 1995). In Arabidopsis, two cryptochromes (cry1 and cry2) and five phytochromes (phyA–phyE) are the major photoreceptors responsible for mediating seedling deetiolation in response to blue/UV-A (320–500 nm) and red/far-red light (600–750 nm), respectively. Among the phytochromes, phyB to phyE predominantly regulate light responses under continuous red and white light, whereas phyA is the primary, if not sole, photoreceptor for far-red light (Neff et al., 2000). These photoreceptors perceive and transduce light signals via distinct intracellular-signaling pathways to modulate nuclear gene expression, leading to adaptive changes at the cell and whole organism levels (Ma et al., 2001).

Molecular and genetic studies in Arabidopsis have identified numerous light-signaling intermediates, including both positive and negative regulators of light signal transduction (for review, see Lin, 2002; Quail, 2002; Wang and Deng, 2004). Although many of the signaling molecules have been characterized at the molecular level, the biochemical function of most signaling intermediates and how they act to transduce light signals are largely unknown. Several lines of evidence suggest that light regulation of plant development is achieved at least in part by modifying responses to the plant hormone auxin (indole-3-acetic acid [IAA]; Tian and Reed, 2001; Nemhauser and Chory, 2002). Many light-regulated developmental processes, such as elongation of hypocotyls, leaf expansion, gravi- and phototropic responses, are also regulated by auxin. For example, auxin promotes hypocotyl elongation in light-grown Arabidopsis seedlings, whereas activation of photoreceptors by light

[1] This work was supported by the Boyce Thompson Institute (set-up funds to H.W.).

* Corresponding author; e-mail hw75@cornell.edu; fax 607–254–1242.

Article, publication date, and citation information can be found at www.plantphysiol.org/cgi/doi/10.1104/pp.105.061572.

leads to inhibition of hypocotyl elongation (Jensen et al., 1998). Light has been shown to affect auxin metabolism, auxin transport, and auxin signaling/response in a number of plant species, including maize (*Zea mays*), tobacco (*Nicotiana plumbaginifolia*), pea (*Pisum sativum*), tomato (*Lycopersicon esculentum* Mill.), and cucumber (*Cucumis sativus*; Walton and Ray, 1981; Iino, 1982; Jones et al., 1991; Behringer and Davies, 1992; Kraepiel et al., 1995; Shinkle et al., 1998). In addition, several AUX/IAA proteins (a group of short-lived, auxin-induced transcriptional regulators) have been shown to directly interact with, and to be phosphorylated by oat (*Avena sativa*) phyA in vitro (Colón-Carmona et al., 2000). Moreover, mutations in several light-signaling components, such as HY5 (a photomorphogenesis-promoting basic leucine zipper [bZIP] transcription factor) and CSN5 (a subunit of the photomorphogenesis-repressing constitutive photomorphogenic 9 [COP9] signalosome), cause altered auxin responses, including apical dominance, hypocotyl growth, lateral-root formation, and gravitropism (Schwechheimer et al., 2001; Cluis et al., 2004). Conversely, exogenous application of auxin or transgenic events causing elevated levels of free auxin leads to increased hypocotyl elongation in the light (Romano et al., 1995; Zhao et al., 2001). Further, gain-of-function mutations in *SHY2/IAA3*, *AXR2/IAA7*, and *AXR3/IAA17* all affect light responses and cause short hypocotyls both in the dark and in the light (Leyser et al., 1996; Kim et al., 1998; Tian and Reed, 1999; Nagpal et al., 2000). These studies suggest that light- and auxin-signaling pathways are intertwined.

In this report, we describe one Arabidopsis mutant isolated in our genetic screening for light-signaling mutants, C9-2, which exhibited a hypersensitive response to far-red, red, and blue light in hypocotyl growth inhibition. Isolation of the responsible gene revealed that it encodes a previously reported ABC (ATP-binding cassette)-type transporter protein, AtMDR1 (Noh et al., 2001). We showed that loss-of-function mutants of *AtPGP1*, the closest homolog of *AtMDR1* in Arabidopsis, also displayed a hypersensitive response to far-red, red, and blue-light inhibition of hypocotyl elongation, though their phenotype is weaker than that of the *atmdr1* mutants. In addition, *atmdr1* and *atpgp1* mutants exhibited defects in accumulation of chlorophyll and anthocyanin, and abnormal expression of several light-responsive genes. We also uncovered roles of these two homologous genes in regulating multiple aspects of root development, including root elongation, lateral-root formation, and root gravitropic response, in the presence or absence of exogenous auxin or an auxin transport inhibitor, naphthylphthalamic acid (NPA). Moreover, our auxin-feeding and auxin-responsive reporter gene studies provided supporting evidence for the notion that AtMDR1 and AtPGP1 participate in auxin efflux required for basipetal auxin transport. Further, we found that mutations in *phyA* largely suppress the randomized-hypocotyl growth and the short-hypocotyl phenotype of the *atmdr1* mutants under far-red light, suggesting that phyA acts downstream of AtMDR1.

## RESULTS

### Isolation of atmdr1 and atpgp1 Mutants

In an effort to isolate additional phyA-signaling mutants, we screened the activation tagging Arabidopsis T-DNA mutant population generated by Dr. Weigel and his colleagues (Arabidopsis Biological Resource Center [ABRC] CS21991, Weigel et al., 2000). One of the mutants isolated, C9-2, exhibited increased responses to continuous far-red light with shorter hypocotyls and more opened cotyledons. Further analysis of this mutant revealed that it is hypersensitive to continuous red and blue light as well. C9-2 dark-grown seedlings reach a similar height as wild-type seedlings with closed cotyledons. Another obvious alteration is the S-shaped waviness of C9-2 mutant hypocotyls (Fig. 1A).

To define the molecular lesion in the C9-2 mutant, we used thermal asymmetric interlaced (TAIL)-PCR (Liu et al., 1995) to amplify the T-DNA flanking sequence. Sequencing analysis of the amplified PCR product revealed that the T-DNA was inserted into the Arabidopsis gene At3g28860 (Fig. 1B), corresponding to the *AtMDR1* gene defined by the Spalding group (Noh et al., 2001), or *AtPGP11* by Philip Rea's group (Sánchez-Fernández et al., 2001), or *AtPGP19* according to the nomenclature of Martinoia et al. (2002). In this study, we followed the Spalding group's nomenclature as the Spalding group reported the isolation and initial characterization of the first two T-DNA insertion mutants of *AtMDR1*, *atmdr1-1* and *atmdr1-2* (Noh et al., 2001). Similar to the C9-2 mutant, both previously reported alleles of *atmdr1* displayed downward-folded, or epinastic, cotyledons under white light (Noh et al., 2001). Thus, the C9-2 mutant likely represents a allele of *AtMDR1*. Segregation analysis revealed that the T-DNA insertion in the *AtMDR1* gene cosegregates with the observed short-hypocotyl and epinastic-cotyledon phenotypes under various light conditions. We renamed the C9-2 mutant as the *atmdr1-100* allele to conform to the nomenclature of Arabidopsis genes. To further confirm that these phenotypes are caused by disruption of the *AtMDR1* gene, we obtained two additional T-DNA insertion lines of *AtMDR1* generated by the Salk Institute (Alonso et al., 2003). PCR-based genotyping confirmed the T-DNA insertions in the *AtMDR1* gene (Fig. 1B). These two lines displayed a similar phenotype to *atmdr1-100* and were designated *atmdr1-101* and *atmdr1-102* (Fig. 1A). Reverse transcription (RT)-PCR analysis showed that in all three alleles, mRNA of *AtMDR1* was not detectable (Fig. 1C), and thus they likely all represent null alleles. The hypersensitive nature of loss-of-function *atmdr1* mutants to various light wavelengths suggests that AtMDR1 acts as a negative regulator of light signaling to promote

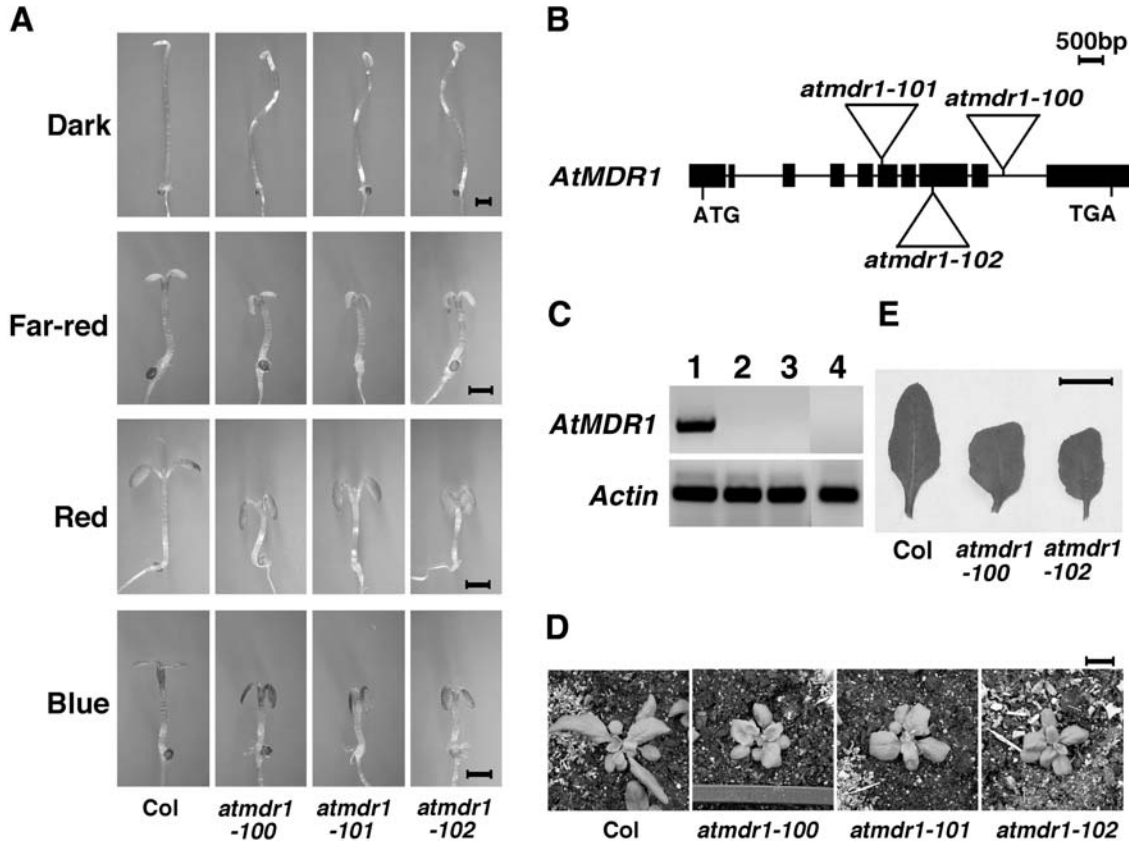


**Figure 1.** Loss-of-function mutants of the *AtMDR1* gene. A, The *atmdr1* mutants have short hypocotyls and epinastic cotyledon under various light conditions and possess wavy hypocotyls in the dark. The seedlings were grown in continuous dark, far-red, red, and blue lights for 4 d. Bar = 1 mm. B, Structure of T-DNA insertion alleles. Black rectangles represent the exons, and lines are introns. Triangles represent T-DNA insertions. C, *AtMDR1* mRNA accumulation is abolished in the T-DNA mutants analyzed by RT-PCR. *Actin* is shown at the bottom as a control. Lane 1, Wild type (Col); lane 2, *atmdr1-100*; lane 3, *atmdr1-101*; lane 4, *atmdr1-102*. D and E, The *atmdr1* mutants have smaller rosettes and their rosette leaves are shorter, but wider, and wrinkled. The plants were grown in soil under long-day conditions (16 h light/8 h dark) at 22°C for 3 weeks. Bar = 1 cm.

hypocotyl elongation. The rosette of adult *atmdr1-100* plants is notably smaller than that of wild-type plants (Fig. 1D), and the mutant leaves were shorter, but wider, and wrinkled along the margin (Fig. 1E).

*AtMDR1* is a member of the *multidrug resistance* (MDR) subfamily of the Arabidopsis ABC transporter gene family. The encoded gene products of this subfamily share a similar topology in having two transmembrane domains connected by a cytoplasmic region containing a nucleotide-binding fold, which is followed by another nucleotide-binding fold near the carboxyl terminus (Sánchez-Fernández et al., 2001). Interestingly, overexpression of *AtPGP1* (At2g36910), the closest homolog of *AtMDR1* in the Arabidopsis genome, was reported to result in longer hypocotyls within a certain range of white-light fluence rates, whereas expression of an antisense construct of *AtPGP1* results in shorter hypocotyls (Sidler et al., 1998). However, a separate study reported that no morphological differences were detected with *atpgp1* loss-of-function mutants (Noh et al., 2001). To resolve the discrepancies regarding *AtPGP1* in regulating hypocotyl elongation, we obtained two T-DNA insertion mutant alleles of *AtPGP1* from Salk lines (Alonso et al., 2003). PCR and sequencing analysis confirmed the T-DNA insertions and cosegregation of the mutant phenotype (see below for details) with the T-DNA insertions (Fig. 2A). RT-PCR analysis detected no *AtPGP1* mRNA accumulation in these lines (Fig. 2B), and we designated these two lines *atpgp1-100* and *atpgp1-101*, to differentiate them from the *atpgp1-1* allele reported previously (Noh et al., 2001). Both *atpgp1-100* and *atpgp1-101* plants showed a clear hypersensitive response to all light wavelengths, although their phenotype is weaker than that of the *atmdr1* mutants, supporting a functional role of *AtPGP1* in regulating hypocotyl elongation (Fig. 2C). Microscopic examination revealed that the shortened hypocotyl length in both *atmdr1* and *atpgp1* mutants is primarily due to a reduction in cell elongation, rather than cell number (data not shown). In contrast with the *atmdr1* mutants, dark-grown *atpgp1* mutant seedlings and *atpgp1* adult plants grown under long-day conditions (16-h light, 8-h dark) were essentially normal (Fig. 2C; data not shown). As reported for the *atmdr1-1/atpgp1-1* double mutant (Noh et al., 2001), the

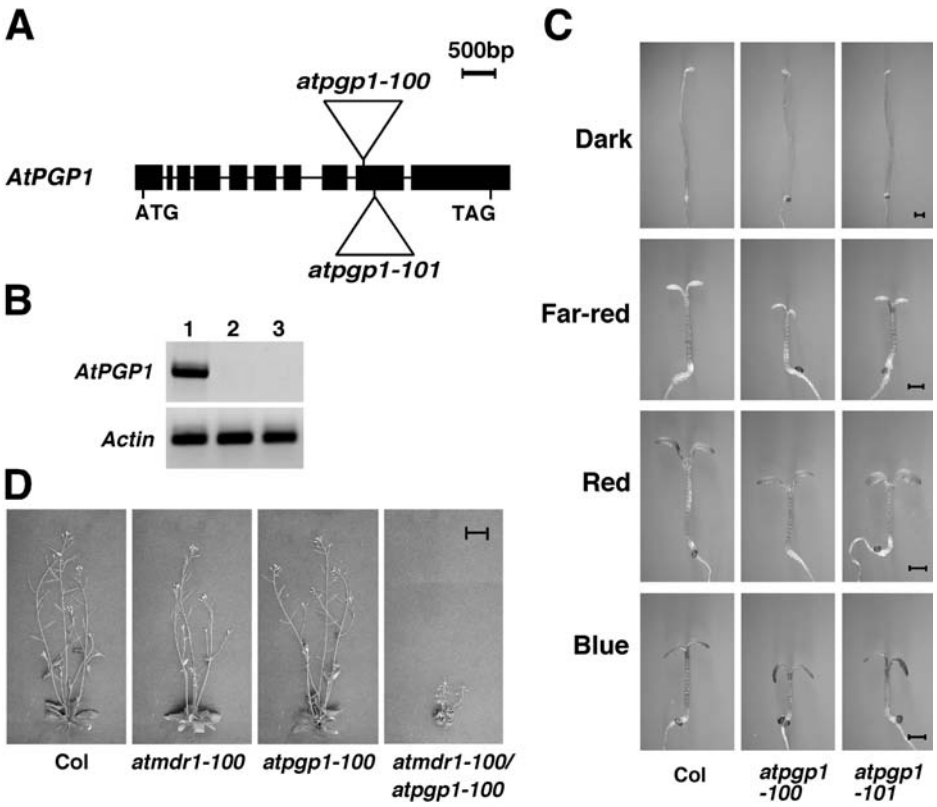


**Figure 2.** Loss-of-function mutants of the *AtPGP1* gene and the *atmdr1-100/atpgp1-100* double mutant. A, Schematic structure of T-DNA insertion alleles. Black rectangles represent the exons, and lines are introns. Triangles represent T-DNA insertions. B, RT-PCR analysis of the *atpgp1* mutants. *Actin* serves as a control. Lane 1, Wild type (Col); lane 2, *atpgp1-100*; lane 3, *atpgp1-101*. C, The *atpgp1* mutants possess shorter hypocotyls under different light conditions but are normal in the dark. The seedlings were grown in continuous dark, far-red, red, and blue lights for 4 d. Bar = 1 mm. D, Four-week old adult plants of wild type (Col), *atmdr1-100*, *atpgp1-100*, and the *atmdr1-100/atpgp1-100* double mutant. Bar = 1 cm.

*atmdr1-100/atpgp1-100* double mutants showed a significantly enhanced dwarfism phenotype (Fig. 2D). These observations indicate that *AtMDR1* and *AtPGP1* have nonredundant, partially overlapping functions.

### Reduced Anthocyanin and Chlorophyll Accumulation, and Abnormal Light-Responsive Gene Expression in *atmdr1* and *atpgp1* Mutants

To affirm that the *atmdr1* and *atpgp1* mutants are defective in light signaling, we measured hypocotyl elongation of the *atmdr1-100* and *atpgp1-100* mutants under a wide range of fluence rates of far-red light. As shown in Figure 3A, both the *atmdr1-100* and *atpgp1-100* mutants retained their responsiveness to various fluence rates of far-red light, but were hypersensitive to far-red light inhibition of hypocotyl elongation under all fluence rates tested, compared to wild-type plants. This result suggests that *AtMDR1* and *AtPGP1* likely define bone fide light-signaling components. In addition, the *atmdr1-100* and *atpgp1-100* mutants accumulated less chlorophyll in seedlings that were grown in continuous far-red light for 3 d then transferred to white light for 2 d to promote chloroplast maturation (Fig. 3B). The reduction in chlorophyll accumulation is consistent with the hypersensitive response of the *atmdr1-100* mutants, as prolonged far-red light treatment impairs subsequent greening upon transferring to white-light conditions (Barnes et al., 1996). Moreover, both the *atmdr1-100* and *atpgp1-100* mutants accumulated less anthocyanin under continuous far-red and blue light (Fig. 3C), suggesting that *AtMDR1* and *AtPGP1* are required for normal accumulation of anthocyanin.

Consistent with the reduced accumulation of chlorophyll and anthocyanin in the *atmdr1-100* and *atpgp1-100* mutants, northern-blot analysis revealed that both mutants had reduced expression levels of *CAB3* (encoding chlorophyll *a/b*-binding protein, required for chlorophyll accumulation) and *CHS* (encoding chalcone synthase, required for anthocyanin accumulation) under both darkness and far-red light. In addition, both mutants also accumulated less *RBCS* (encoding small subunit of riboluse-1,5-biphosphate carboxylase) and *PORA* (encoding NADPH:pchlide oxidoreductase A) in these light conditions, and expression of these genes was further reduced in their double mutants (Fig. 4, A–E). This result supports that *AtMDR1* and *AtPGP1* play similar roles in regulating light signaling. Interestingly, northern-blot analysis revealed that the expression of *AtMDR1* itself appears to be light regulated, being slightly repressed by far-red light, but slightly induced by red light. Consistent with this finding, *AtMDR1* expression was found to be elevated in far-red light-grown *phyA-211* mutants (Fig. 4, F and G), suggesting that far-red light inhibition of hypocotyl elongation could involve a phyA-dependent reduction of *AtMDR1* expression.

### *atmdr1* and *atpgp1* Mutants Affect Root Elongation

Previous studies suggested that both AtMDR1 and AtPGP1 participate in auxin transport, based on

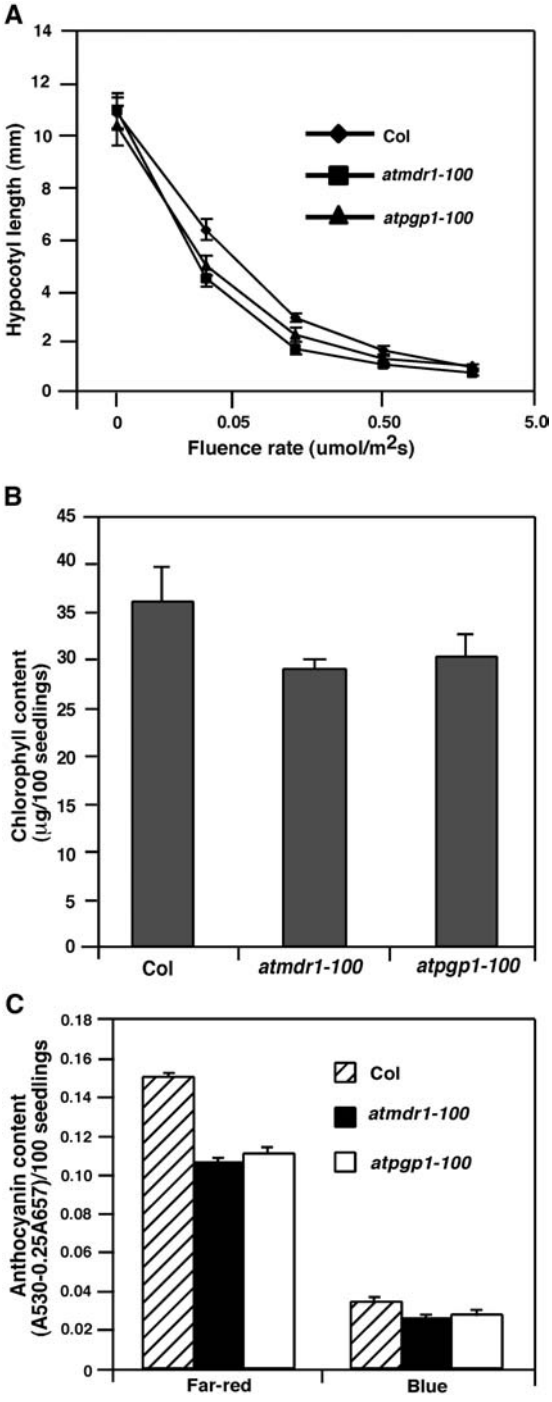


**Figure 3.** Photomorphogenic defects of *atmdr1-100* and *atpgp1-100* mutants. A, Fluence rate responses of 4-d-old *atmdr1-100*, *atpgp1-100*, and wild-type (Col) seedlings under darkness or continuous far-red light. Bars denote SDs from 20 seedlings. B, Chlorophyll content of *atmdr1-100*, *atpgp1-100*, and wild-type (Col) plants. Seedlings were grown in far-red light for 3 d, and then were transferred to white light for 2 d before chlorophyll extraction. Bars represent SDs from triplicate experiments. C, Anthocyanin content of *atmdr1-100*, *atpgp1-100*, and wild-type (Col) plants. Seedlings (approximately 100) were grown in continuous far-red or blue light for 4 d before anthocyanin extraction. Bars represent SDs from triplicate experiments.

assays of measuring the basipetal movement of $^{14}$C-IAA or $^{3}$H-IAA (Noh et al., 2001; Geisler et al., 2003). To reveal additional biological functions of these two homologous genes and to substantiate their role in auxin transport, we tested the effects of *atmdr1* and *atpgp1* mutations on three hallmark responses mediated by auxin: root elongation, lateral-root formation, and root gravitropic growth. On unsupplemented media, root elongation of the *atmdr1-100*, *atpgp1-100*, and *atmdr1-100/atpgp1-100* mutants was essentially normal, like that of wild-type plants (data not shown). Interestingly, differential responsiveness of *atmdr1-100*, *atpgp1-100*, and their double mutant to exogenously supplied auxin was observed. Although both the *atmdr1-100* and *atpgp1-100* single mutants responded to the synthetic auxin 2,4-dichlorophenoxyacetic acid (2,4-D, an influx substrate) similarly to wild-type plants, their double mutant displayed slightly reduced root elongation at low concentrations (such as 10 nM) of 2, 4-D (Fig. 5A). Moreover, the *atmdr1-100* single mutant, and especially the *atmdr1-100/atpgp1-100* double mutants, showed clearly increased sensitivity to 1-naphthalene acetic acid (1-NAA, an efflux substrate) inhibition of root elongation, although the *atpgp1-100* mutant roots responded to 1-NAA normally as did wild-type plants (Fig. 5B). The differential sensitivities to 1-NAA and 2,4-D suggest that AtMDR1 and AtPGP1 likely participate in auxin efflux. It is anticipated that loss or reduction in auxin efflux activity would cause an accumulation of its substrate 1-NAA in plant cells, leading to greater sensitivity toward this auxin analog. Consistent with this defect, the *atmdr1-100* and *atmdr1-100/atpgp1-100* mutants were less sensitive to NPA inhibition of root elongation (Fig. 5C). The *atpgp1-100* mutant also showed reduced sensitivity to low concentrations (such as 0.1 $\mu$M) of NPA. Similar differential responses to 1-NAA and NPA have been reported with the auxin efflux mutant *agr1/atpin2* (Chen et al., 1998; Müller et al., 1998).

### *atmdr1* and *atpgp1* Mutants Affect Lateral-Root Formation

Basipetal transport of auxin from the shoot apex into the roots is required for promoting lateral-root formation (Casimiro et al., 2001). To examine whether AtMDR1 and AtPGP1 are required for auxin-mediated lateral-root formation, we examined their effects on lateral-root formation in the presence or absence of exogenous auxin. When grown vertically on unsupplemented media, both *atmdr1-100* and *atpgp1-100* mutants possessed fewer lateral roots than did wild-type control plants, and the *atmdr1-100/atpgp1-100* double mutant had further reduced lateral roots (Fig. 5D). When grown on media supplemented with 2,4-D (100 nM) for 4 d, the single and double mutants responded normally as did wild-type plants. However, on the media supplied with 1-NAA (100 nM) or NPA (0.1 $\mu$M), the mutants still produced fewer lateral roots per primary root than wild-type plants (Fig. 5D).

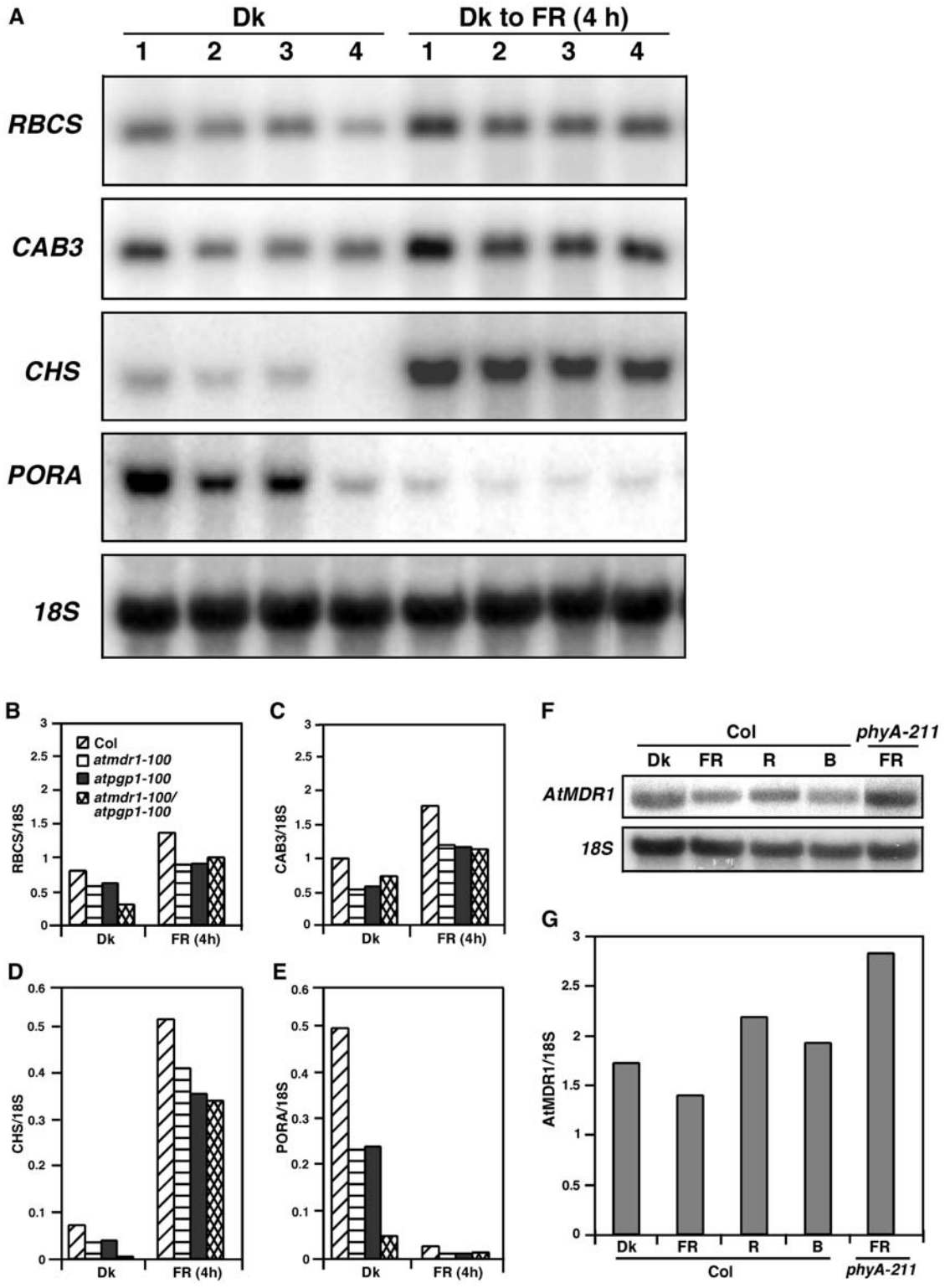


**Figure 4.** Abnormal expression of light-responsive genes in the *atmdr1-100* and *atpgp1-100* mutants. A, Reduced expression of *RBCS, CAB3, CHS,* and *PORA*. RNAs were extracted from seedlings grown in darkness (Dk) for 4 d, or seedlings grown in darkness for 4 d then exposed to far-red (FR) for 4 h. An *18S* rRNA blot of the duplicating gels was shown below as a loading control. Lane 1, Col; lane 2, *atmdr1-100*; lane 3, *atpgp1-100*; lane 4, *atmdr1-100/atpgp1-100*. B to E, Relative expression levels of light-responsive genes quantified with a PhosphorImager, normalized against *18S* rRNA. F, Light regulation of *AtMDR1* expression. Wild-type (Col) or *phyA-211* mutant seedlings were grown in continuous darkness (Dk), far-red (FR), red (R), or blue (B) for 4 d before total RNA extraction. An *18S* rRNA blot was shown as a loading control. G, Relative *AtMDR1* expression levels quantified with a PhosphorImager. The expression levels were normalized against *18S* rRNA.

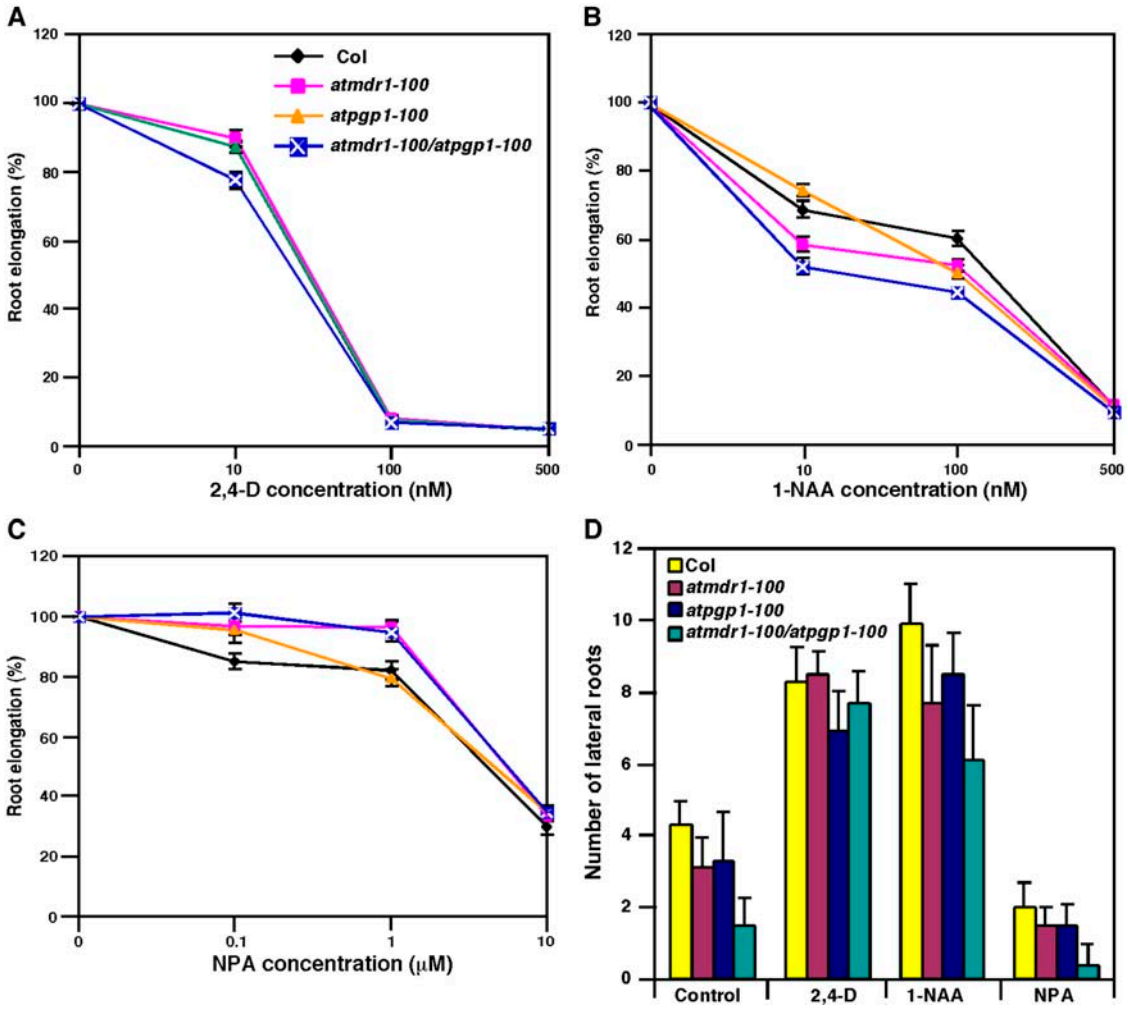


**Figure 5.** *atmdr1* and *atpgp1* affect root elongation and lateral-root formation. Seedlings were grown vertically on germination plates for 3 d under white light and then transferred to new unsupplemented plates or plates supplemented with various hormones. A to C, Relative root elongation of wild type (Col), *atmdr1-100*, *atpgp1-100*, and *atmdr1-100/atpgp1-100* mutants on plates supplemented with various concentrations of 2,4-D, 1-NAA, and NPA for 4 d, respectively. The percentage of relative root elongation was calculated based on control plants grown on unsupplemented media. Bars indicate the SDS from 20 to 25 seedlings. The plant genotypes for A to C are indicated in A. D, Lateral root number of wild type (Col), *atmdr1-100*, *atpgp1-100*, and *atmdr1-100/atpgp1-100* mutants on medium with or without 100 nM 1-NAA, 100 nM 2,4-D, and 0.1 $\mu$M NPA. Bars indicate the SDS from 20 to 25 seedlings.

Thus, neither 1-NAA nor NPA was able to rescue the lateral-root defect of the *atmdr1-100*, *atpgp1-100*, and *atmdr1-100/atpgp1-100* mutants. These results suggest that AtMDR1 and AtPGP1 are required for basipetal auxin transport from shoot apex into the root necessary for normal lateral-root formation.

To provide further evidence that AtMDR1 participates in auxin efflux required for basipetal auxin transport in the roots, we introduced the auxin-responsive reporter gene *DR5*::*GUS* into the *atmdr1-100* mutant background to examine the effects of three different auxins (IAA, 1-NAA, and 2,4-D) and the auxin efflux inhibitor NPA on *DR5*::*GUS* reporter gene expression pattern in wild type and the *atmdr1-100* mutants. Auxin or NPA was applied to either the hypocotyl-root junction sites or root tips of whole seedlings for 3 h and then $\beta$-glucuronidase (GUS) staining was conducted. No notable differences were detected between wild type and the *atmdr1-100* mutant roots when auxin or NPA was applied at the hypocotyl-root junction sites (data not shown), suggesting that auxin acropetal transport into the roots was not affected in the *atmdr1-100* mutants. In addition, no differences were detected when IAA or 2,4-D was applied to the root tips (Fig. 6A). However, GUS staining in the central elongation zone was much stronger in wild-type roots exposed to 1-NAA at the root tips (Fig. 6A). This result supports the proposition that AtMDR1 is required for auxin basipetal transport from the root tip to the central elongation zone.

Previously, using the *DR5*::*GUS* reporter gene, it was shown that NPA could cause accumulation of free IAA

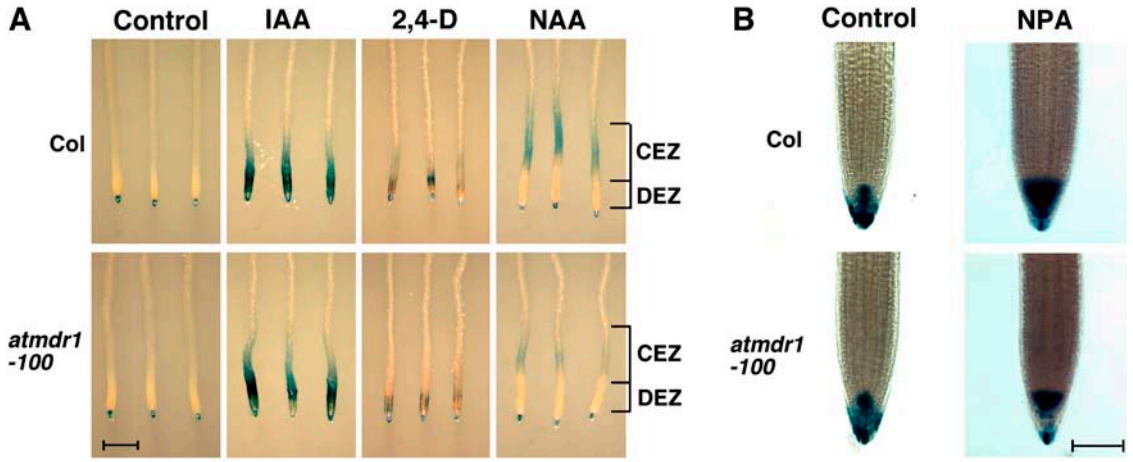


**Figure 6.** Effects of hormone treatments on *DR5*::*GUS* expression. GUS staining of root tips of wild-type (Col) and *atmdr1-100* seedlings harboring the *DR5*::*GUS* reporter gene. Seedlings were first grown vertically on germination plates for 4 d and then subjected to hormone treatments and GUS staining. A, Seedlings were treated with IAA (1.0 $\mu$M), 1-NAA (1.0 $\mu$M) or 2,4-D (1.0 $\mu$M) at the root tips for 3 h. Bar = 1 mm. CEZ, Central elongation zone; DEZ, distal elongation zone. B, Seedlings were treated with or without NPA (2.0 $\mu$M) for 24 h. Bar = 100 $\mu$m.

in the root tips, leading to GUS staining of larger areas of root apex (Casimiro et al., 2001). We examined the effects of NPA on GUS-staining patterns in both wild type and the *atmdr1-100* mutants. The GUS expression domains in untreated wild type and the *atmdr1-100* mutant roots were essentially identical with expression in the columella and lateral-root cap cells. NPA treatment significantly increased the expression domains of *DR5*::*GUS* in wild-type roots, whereas the GUS expression domain in the *atmdr1-100* mutant roots was much smaller (Fig. 6B). This result suggests that the *atmdr1-100* mutants are less sensitive to NPA inhibition of auxin transport and accumulate relatively less free auxin in the root apex than do wild-type plants.

### *atmdr1* and *atpgp1* Affect Root Gravitropism

Tropic growth is believed to involve asymmetric auxin transport that leads to differential elongation on opposite sides of an organ (Rashotte et al., 2000). It is expected that the *atmdr1* and *atpgp1* mutants may have impaired gravitropism due to a reduction of polar auxin transport (PAT). Surprisingly, a recent study showed the *atmdr1-1* and *atmdr1-1/atpgp1-1* double mutants exhibited much enhanced phototropic and gravitropic growth of hypocotyls (Noh et al., 2003). To determine whether AtMDR1 and AtPGP1 are involved in root gravitropic response, *atmdr1-100*, *atpgp1-100*, *atmdr1-100/atpgp1-100* double mutant, and wild-type control plants were grown in dark for 2 d and then rotated 90 degrees. The angle changes were measured every 6 h over a 24-h period. As shown in Figure 7, the *atmdr1-100* mutant roots displayed a faster response to gravity stimulus than wild-type plant roots, while the response of *atpgp1-100* mutant roots was essentially normal. Roots of the *atmdr1-100/atpgp1-100* double mutant exhibited more enhanced gravitropic response than the roots of *atmdr1-100* single mutant within the first 12 h of gravity stimulation (Fig. 7, A and B).

To explore the cellular mechanism of enhanced gravitropism in the *atmdr1-100* mutant roots, we examined whether the enhanced root gravitropism of the *atmdr1-100* mutant correlates with the development of a lateral-auxin gradient, using the auxin-responsive *DR5*::*GUS* reporter gene. Upon gravistimulation, both wild type and the *atmdr1-100* mutant roots produced an asymmetric pattern of GUS staining across the root tip; however, the *atmdr1-100* mutant roots formed an asymmetric GUS-staining pattern earlier than did wild-type roots. At 3 h after the gravistimulation, approximately 63% (10 out of 16) *atmdr1-100* mutant roots and 33% of wild-type roots (6 out of 18) developed clearly visible asymmetric GUS-staining patterns at the lower side of the root distal elongation zone (Fig. 7, C and D). At 5 h after the reorientation, this asymmetric GUS-staining pattern was seen in approximately 71% (15 out of 21) *atmdr1-100* mutant roots and 68% of wild-type roots (13 out of 19), and the staining was stronger and wider with the *atmdr1-100* mutant roots (Fig. 7E). Interestingly, 8 h after the reorientation, roots with asymmetric GUS-staining patterns were reduced to approximately 40% for both wild type and the *atmdr1-100* mutant, indicating a decay of auxin levels. These results suggest that the *atmdr1-100* mutants might be defective in basipetal transport of auxin from the distal elongation zone to the central elongation zone, causing an accumulation of auxin in the distal elongation zone and more lateral-auxin transport in this region, which leads to enhanced root gravitropism. NPA treatment blocked both gravitropic bending and formation of the asymmetric *DR5-GUS* expression pattern in both wild type

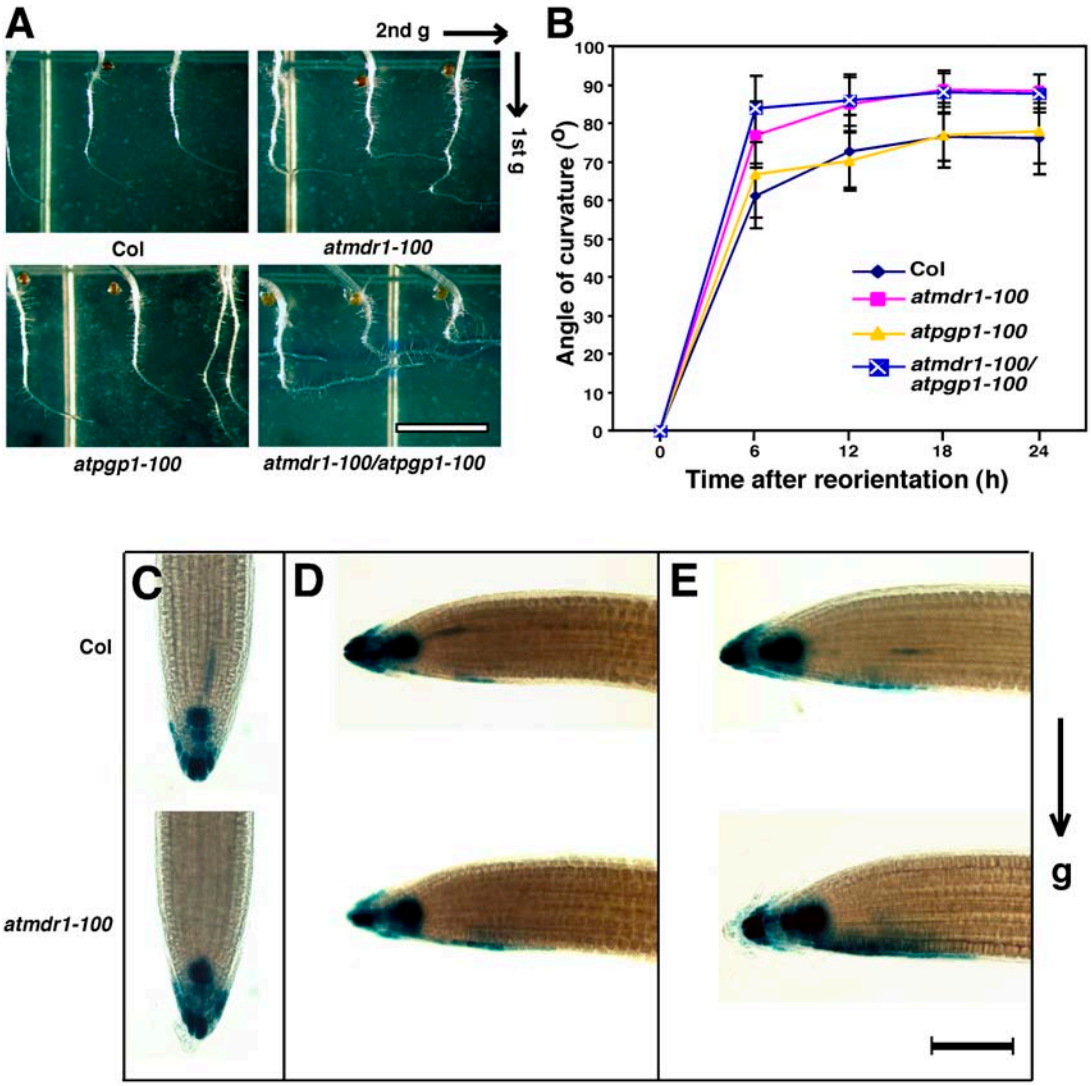


**Figure 7.** Enhanced gravitropic responses of the *atmdr1* and *atmdr1/atpgp1* double mutant. A, Representative root images of wild-type (Col), *atmdr1-100*, *atpgp1-100*, and *atmdr1-100/atpgp1-100* mutant seedlings 24 h after gravistimulation. Seedlings were grown vertically on unsupplemented germination plates in darkness for 2 d, and then the plates were rotated 90°. Bar = 1 cm. Arrows indicate the gravity vector. B, Time course of root gravitropic response. The angles of curvature were measured every 6 h over a 24-h period. Bars indicate SDs from 35 to 40 seedlings. C to E, GUS staining of seedlings 0 (before gravistimulation), 3, and 5 h after reorientation, respectively. Seedlings of wild type (Col) and *atmdr1-100* mutant harboring *DR5*::*GUS* reporter gene were grown vertically on germination plates under white light for 4 d, and then were transferred to new plates for 24 h. The plates were then rotated 90°. At the indicated times, seedlings were harvested for GUS staining. Bar = 100 $\mu$m. Arrow indicates the gravity vector.

and the *atmdr1-100* mutants (data not shown), supporting the notion that development of an asymmetric GUS-staining pattern in the root distal elongation zone is a prerequisite for gravitropic growth of roots.

### Characterization of *atmdr1-100*/*axr1-3* Double Mutants

The pleiotropic nature of *atmdr1* mutants shares much similarity to the *axr1* mutants. The *axr1* mutants show reduced auxin responses and are characterized by a reduction in stature and wrinkled, irregularly shaped leaves, reduced lateral-root formation, and reduced root gravitropism (Lincoln et al., 1990). The *AXR1* gene encodes a subunit of the E1 enzyme involved in conjugation of the ubiquitin-like protein RUB1 to CUL1 and is essential for normal auxin responses (Dharmasiri and Estelle, 2004). To determine whether AtMDR1 and AXR1 interact to facilitate auxin response, *atmdr1-100/axr1-3* double mutants were constructed and analyzed. The hypocotyl lengths of dark-grown *atmdr1-100*, *axr1-3*, and *atmdr1-100/axr1-3* mutant seedlings were essentially normal; however, the hypocotyls of light-grown *atmdr1-100* and *axr1-3* single-mutant seedlings were shorter than that of

wild-type plants, and their double mutants had further reduced hypocotyl lengths, suggesting an additive effect of these two mutations on hypocotyl elongation (Fig. 8A). Strikingly, the rosettes of the double mutants were significantly smaller than either single-parental mutant (Fig. 8B). Moreover, the adult double mutant plants exhibited severe dwarfism, with a phenotype much more severe than either single-parent mutant (Fig. 8C). These results suggest that AtMDR1 and AXR1 act synergistically in regulating the development of aboveground organs, and support the notion that AtMDR1 is involved in regulating auxin-dependent growth in multiple tissues.

### phyA Acts Downstream of AtMDR1 in Regulating Hypocotyl Elongation and Gravitropic Response

The observed defects of the *atmdr1-100* mutant in both photomorphogenesis and auxin transport promoted us to test the epistatic relationship between auxin transport and light signaling. We generated an *atmdr1-100/phyA-1* double mutant and examined its responses to NPA treatment in comparison to their single-parental mutants. Under continuous far-red light, NPA severely inhibited hypocotyl elongation of wild-type seedlings, but it inhibited hypocotyl elongation of the *atmdr1-100* mutants to a much lower degree. Interestingly, NPA had a minimal effect on hypocotyl elongation in the *phyA-1* mutants, although it disrupted the apical hook formation of the *phyA-1* mutants. Strikingly, the hypocotyl of the *atmdr1-100/phyA-1* double mutant elongated essentially similar to the *phyA-1* single mutant, with or without NPA treatment (Fig. 9, A and B). This result suggests that active phyA is required for the far-red light-dependent short-hypocotyl phenotype of the *atmdr1* mutants and that phyA acts downstream of AtMDR1.

To provide further evidence for such an epistasis relationship between AtMDR1 and phyA, we examined hypocotyl negative-gravitropism response of *atmdr1-100*, *phyA-1*, and their double mutants. Wild-type plants of both the Columbia (Col) and Landsberg *erecta* (L*er*) ecotypes and the *phyA-1* mutants displayed strong negative gravitropism in the dark, whereas the *atmdr1-100* and the *atmdr1-100/phyA-1* double mutants exhibited slightly increased randomization of hypocotyl growth. Both wild-type plants and the *atmdr1-100* mutants displayed highly randomized-hypocotyl growth under continuous far-red light, whereas randomized-hypocotyl growth was essentially blocked in the *phyA-1* single mutants and the *atmdr1-100/phyA-1* double mutants (Fig. 9C). This observation suggests that the *phyA-1* mutation is epistatic to the *atmdr1-100* mutation in mediating hypocotyl growth orientation under far-red light.

We also examined root growth inhibition of *atmdr1-100*, *phyA-1*, and their double mutants in the absence or presence of exogenous auxin, under continuous far-red light. As shown in Figure 9D, on unsupplemented media, elongation growth of the *atmdr1-100* mutant roots was comparable to its corresponding wild-type plants (Col), whereas the *phyA-1* mutant roots elongated slightly slower than its corresponding wild-type plant (L*er*). Interestingly, elongation growth of their double mutants was further reduced, compared to the *phyA-1* single mutants. On growth media supplied with 10 nM or 100 nM of 1-NAA, elongation growth of both the *atmdr1-100* and *phyA-1* mutant roots was reduced, compared to their respective wild-type plants. More pronounced reductions in root elongation were observed for their double mutants on supplemented media, suggesting an additive effect of these two mutations. Together, these results indicate that the genetic interaction between phyA and AtMDR1

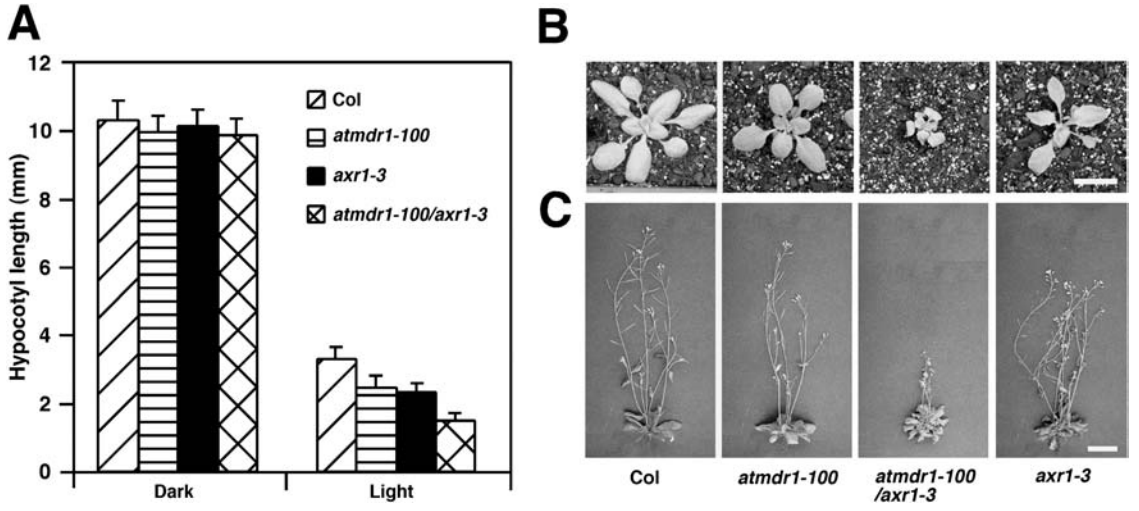


**Figure 8.** Characterization of the *atmdr1-100/axr1-3* double mutant. A, Hypocotyl length of wild type, *atmdr1-100*, *axr1-3*, and *atmdr1-100/axr1-3* mutants in continuous darkness or white light for 4 d. Bars represent SDs from 20 seedlings. B and C, Eighteen- and 28-d-old plants grown in soil, respectively. Bar = 1 cm.

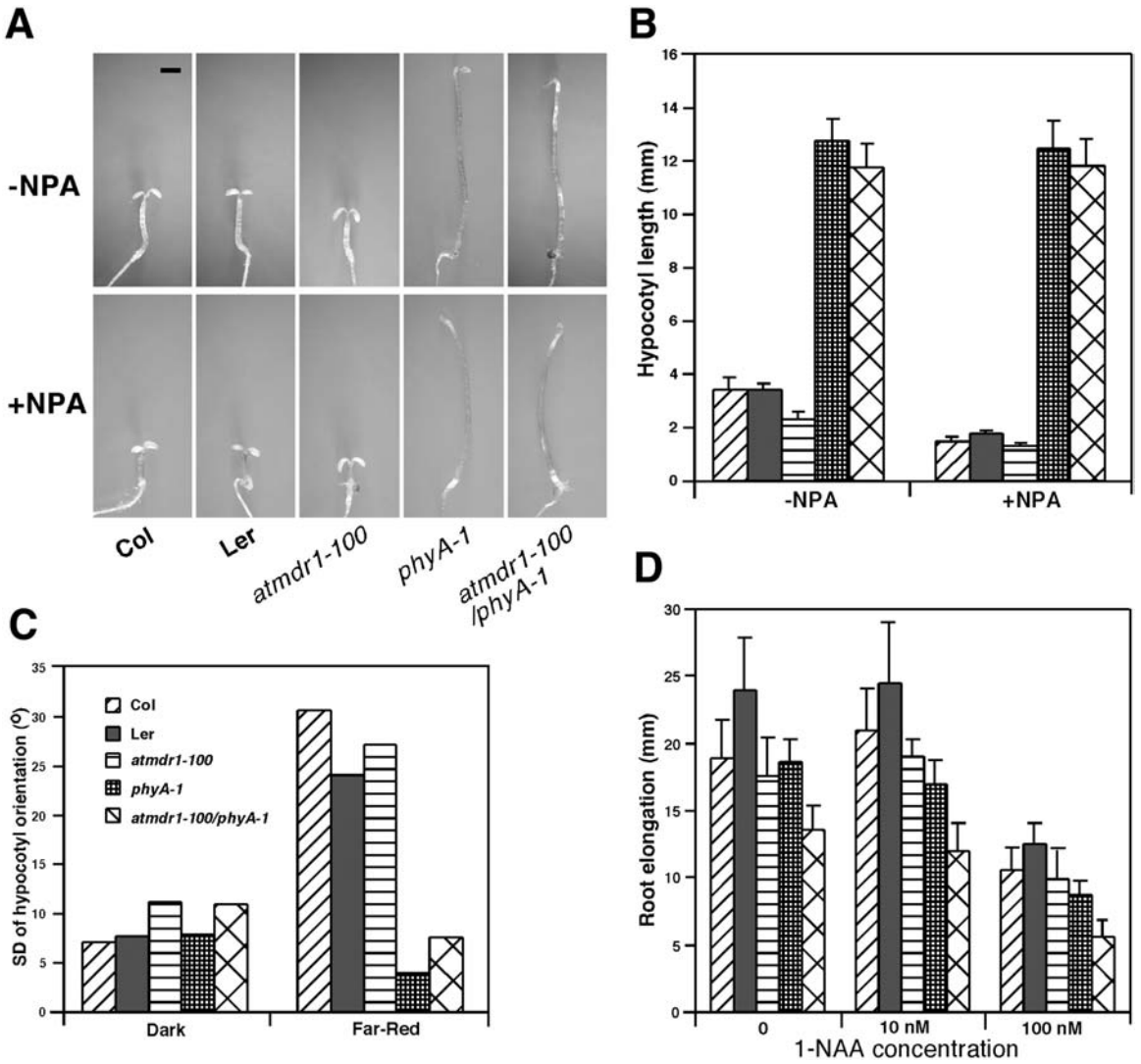


**Figure 9.** phyA acts downstream of AtMDR1 in regulating hypocotyl growth. A, Representative pictures of wild type (Col, L*er*), *atmdr1-100*, *phyA-1* single mutants, and *atmdr1-100/phyA-1* double mutant grown on germination plates with or without 2.0 $\mu$M NPA under far-red light for 4 d. Bar = 1 mm. B, Hypocotyl length of wild type (Col, L*er*), *atmdr1-100*, *phyA-1*, and *atmdr1-100/phyA-1* as shown in A. Bars represent SDs from 20 seedlings. C, Hypocotyl orientation of Arabidopsis seedlings grown in the darkness or continuous far-red light for 5 d. The orientation of hypocotyls angle was measured as the SD around the vertical 0°. Values represent the pooled SD for a minimum of 100 seedlings from triplicate experiments. High SDs indicate randomization of hypocotyls. D, Root elongation of wild type (Col, L*er*), *atmdr1-100*, *phyA-1*, and *atmdr1-100/phyA-1* mutants under far-red light. Seedlings were vertically grown in far-red for 3 d and then transferred to new plates with (10 nM or 100 nM) or without 1-NAA for further 4 d before the additional root elongation was measured. Bars denote SDs from 20 seedlings. For B to D, the plant genotypes are shown in C.

is complex, and might be tissue or response type dependent.

## DISCUSSION

### AtMDR1 and AtPGP1 Regulate Photomorphogenesis in Arabidopsis

In this study, we conducted functional characterization of *AtMDR1* and *AtPGP1* genes based on mutant alleles identified from our genetic screen for light-signaling mutants. Multiple alleles of loss-of-function *atmdr1* and *atpgp1* mutants showed a hypersensitive response to far-red, red, and blue-light inhibition of hypocotyl elongation, although the *atmdr1* mutants had a stronger phenotype than the *atpgp1* mutants in this regard. In addition, these mutants displayed a hypersensitive response to a wide range of fluence rates of far-red light, supporting that *AtMDR1* and *AtPGP1* might represent authentic light-signaling intermediates. Moreover, both the *atmdr1-100* and *atpgp1-100* mutants accumulated less chlorophyll and anthocyanin, and had reduced expression levels of

a number of light-responsive genes, including *CAB3*, *RBCS*, *CHS*, and *PORA*, under both darkness and far-red light. These results suggest the *AtMDR1* and *AtPGP1* share similar functions in regulating light signaling. They could act either to promote certain branches of light-signaling pathway (such as chlorophyll and anthocyanin accumulation) or inhibit some other branches of light-signaling pathway (such as hypocotyl growth inhibition and down-regulation of *PORA* expression).

Notably, a number of phenotypes were seen only with the *atmdr1-100* mutant, including epinastic cotyledons in light-grown seedlings, wavy hypocotyls of dark-grown seedlings, smaller rosettes with epinastic leaves, and enhanced root gravitropism. However, it is likely that *AtPGP1* also participates in these processes, as epinastic cotyledons, enhanced hypocotyl and root gravitropism, and the dwarfism phenotype of adult plants were seen in the *atmdr1/atpgp1* double mutants (Noh et al., 2003; this study). These results suggest that AtMDR1 and AtPGP1 are required for normal growth and development in multiple Arabidopsis tissues. Interestingly, previous studies have demonstrated that *AtMDR1* is expressed more or less ubiquitously, including seedlings, roots, rosette leaves, flowers, and aboveground tissues before bolting (Noh et al., 2001), whereas expression of *AtPGP1* seems to be limited to shoot apices and root tips (Sidler et al., 1998). Thus, the morphological abnormalities of the *atmdr1* and *atpgp1* mutants are in general agreement with their expression patterns. For example, expression of *AtPGP1* was not detected in the cotyledons of light-grown seedlings (Sidler et al., 1998), consistent with the lack of notable epinastic phenotype of cotyledons in the *atpgp1* mutants. However, the much-enhanced phenotype displayed by the *atmdr1/atpgp1* double mutants suggests nonreciprocal functional redundancy between *AtMDR1* and *AtPGP1*.

AtMDR1 and AtPGP1 are the two closest homologs within the Arabidopsis ABC transporter gene family. One major function of plant ABC transporters is to detoxify cells through vacuolar sequestration of various metabolites or excretion of toxic compounds out of the cells (Martinoia et al., 2002). Interestingly, overexpression of *AtPGP1* has been recently shown to result in increased resistance to herbicides from different chemical classes, possibly by decreasing the retention or increasing active efflux of herbicide from the plant cells, supporting multifunctionality of AtPGP1 (Windsor et al., 2003). Genetic analysis of loss-of-function mutants of several other Arabidopsis ABC transporter genes has revealed their diverse roles in plant growth and development, including metabolite translocation, light response, stomata movement, auxin transport, maturation of cytosolic Fe/S proteins, drought resistance, and seed maturation. For example, mutations in an ABC transporter, LAF6, cause reduced responsiveness toward continuous far-red light (Møller et al., 2001). Both AtMDR4 and AtMDR5 regulate stomatal opening, and AtMDR5 is also involved in the regulation of root development (Gaedeke et al., 2001; Klein et al., 2003, 2004). In addition, mutations in the *AtMDR1* orthologs in maize and sorghum (*Sorghum bicolor*; *br2* and *dw3*, respectively) also result in defects in growth, causing compact stalks (Multani et al., 2003). It will be of high interest to reveal the functions of other related ABC transporters in regulating Arabidopsis development in the future using available forward and reverse genetic approaches.

### Roles of AtMDR1 and AtPGP1 in Modulating Auxin Efflux

Auxin is primarily synthesized in the shoot apex and young developing organs, and is transported to sites of its action in the basal regions of shoots and roots via a specialized PAT system (Friml and Palme, 2002; Muday and Murphy, 2002). Recent molecular genetic studies of Arabidopsis mutants defective in PAT have lead to the identification and characterization of auxin transport proteins. For example, AUX1, an amino acid permease-related protein, likely acts as a membrane-integrated auxin influx carrier (Marchant et al., 1999). A group of PIN proteins encoded by a multigene family comprising *AtPIN1-AtPIN8* shares similarity to bacterial-type transporters and are potential transmembrane auxin efflux carriers (Friml and Palme, 2002; Muday and Murphy, 2002). Previous studies also implicated AtMDR1 and AtPGP1 in auxin transport based on NPA binding and auxin transport assays in the *atmdr1-1* and *atmdr1-1/atpgp1-1* double mutants (Noh et al., 2001; Murphy et al., 2002).

In this study, we showed that in addition to their hypersensitivity to light inhibition of hypocotyl elongation, *atmdr1-100*, *atpgp1-100*, and their double mutants have pleiotropic defects in root development as well. We showed that both the *atmdr1-100* and *atmdr1-100/atpgp1-100* double mutants were more sensitive to 1-NAA inhibition of root elongation and less sensitive to NPA inhibition of root elongation. In addition, the *atmdr1-100* and *atpgp1-100* mutants and their double mutants produced fewer lateral roots (with or without treatments of 1-NAA and NPA) and exhibited enhanced root gravitropism. Similar developmental defects have been reported for the Arabidopsis *agr1* and *tir3/big* mutants; both mutations have been suggested to be defective in auxin efflux (Ruegger et al., 1997; Chen et al., 1998; Gil et al., 2001). Further, the finding that expression of the auxin-responsive *DR5*::*GUS* reporter gene in the central elongation zone was significantly reduced in the *atmdr1-100* mutant roots treated with 1-NAA at the root tips (but not in roots treated with 2,4-D) compared to similarly treated wild-type plants, suggests that AtMDR1 is required for normal basipetal auxin transport from the root tip to the central elongation zone.

Our studies also provided additional evidence to support the Cholodny-Went theory of tropism, which hypothesized that upon gravistimulation, lateral-auxin redistribution across the root tips is altered to

form a lateral-auxin gradient, which would then be transported basipetally to the responding elongation zones to promote downward tip curvature (Rashotte et al., 2001; Ottenschläger et al., 2003). We observed a higher percentage of *atmdr1-100* mutant roots developed a stronger asymmetric *DR5*::*GUS*-staining pattern at the root tip in the first 5 h after gravistimulation. This feature correlated well with the enhanced gravitropic growth of the *atmdr1-100* mutant roots. As with our observations, it has been reported that the *rcn1* mutants, which exhibit reduced protein phosphatase 2A activity, display increased root basipetal IAA transport in the root tips, significantly delayed asymmetric *DR5*::*GUS* expression in gravity-stimulated roots, and a delayed gravitropic response (Rashotte et al., 2001). Similarly, the *agr1/eir1/atpin2* mutants have substantially elevated auxin levels in the root tips due to impaired basipetal auxin transport and a delayed gravitropic response (Ottenschläger et al., 2003).

It is not yet clear how AtMDR1 and AtPGP1 participate in auxin transport. One possibility is that they could function together with ion channels and other regulatory proteins to create efficient, NPA-sensitive auxin efflux complex (Noh et al., 2001). Supporting evidence for this notion came from a study showing that AtMDR1 and AtPGP1 can physically interact with the FK506-binding protein (FKBP)-like immunophilin *Twisted Dwarf1*, and that they colocalize onto the plasma membrane. Further, the *twd1-1* single mutant and the *atpgp1-1/atmdr1-1* double mutants exhibit similar phenotypes including epinastic growth, reduced inflorescence size, and reduced PAT, suggesting that *Twisted Dwarf1* functions together with, and possibly modulates the activities of, AtPGP1 and AtMDR1 in regulating auxin efflux and Arabidopsis development (Geisler et al., 2003). It has also been suggested that AtMDR1 and AtPGP proteins may modulate the effects of flavonoids on PIN expression and protein localization, as their activity is flavonoid sensitive (Murphy et al., 2002; Noh et al., 2003). Studying the interactions and functional relationships between AtMDR1 (and its related homologs) with other defined or putative auxin efflux carrier proteins (such as PINs) and their regulatory proteins will certainly lead to a better understanding of the mechanisms regulating PAT.

### phyA Acts Downstream of AtMDR1 in Regulating Elongation and Gravitropic Growth of Hypocotyls

The overlapping functions of light and auxin in regulating multiple developmental processes, such as tropic growth, hypocotyl elongation, and shade avoidance responses, imply functional interactions between their signaling pathways. Accumulating evidence suggests that light could modulate auxin responses by causing changes in auxin production, auxin transport, and auxin signal transduction (Tian and Reed, 2001; Swarup et al., 2002). For example, phytochrome has been shown to regulate the biosynthesis or metabolism of auxin in maize and tobacco (Iino, 1982; Kraepiel et al., 1995). In addition, there are reports that light regulates auxin transport in pea and cucumber seedlings (Behringer and Davies, 1992; Shinkle et al., 1998). Light regulation of auxin transport likely involves the induced production of flavonoids, which act to inhibit auxin transport (Buer and Muday, 2004). In addition, some other recent studies suggested that phytochrome might regulate auxin transport through altering the expression of the *ATHB-2* gene, which encodes a homeodomain Leu zipper protein required for shade avoidance response (Steindler et al., 1999). Together, these studies support the proposal that PAT represents a target for light-signaling pathways to regulate photomorphogenesis.

There is also evidence suggesting a regulatory role of auxin transport on light signaling. The observation that NPA inhibits hypocotyl elongation by blocking PAT in light-grown Arabidopsis seedlings, but not on dark-grown seedlings, suggests that light is required for the inhibitory role of NPA on hypocotyl elongation. Further, analysis of photoreceptor mutants indicates the involvement of phytochrome and cryptochrome in mediating this NPA response (Jensen et al., 1998). Another recent work showed that the *doc1/tir3/big* mutants express light-regulated genes in the dark and have decreased auxin transport rates. Interestingly, the aberrant light-regulated gene expression in this mutant can be largely suppressed by an increase in the endogenous auxin levels, suggesting that proper auxin transport (or auxin signaling) plays an important role in repressing light-regulated gene expression in the dark (Ruegger et al., 1997; Gil et al., 2001). Consistent with this notion, we showed in this study that *AtMDR1* and *AtPGP1* are required for proper expression of several light-responsive genes including *CAB3*, *RBCS*, *CHS*, and *PORA*, under both darkness and far-red light. In addition, the finding that the hypocotyl of *atmdr1-100/phyA-1* double mutant elongated essentially as the *phyA-1* single mutant under far-red light, with or without NPA treatment, suggests that active phyA is required for the far-red light-dependent short-hypocotyl phenotype of the *atmdr1-100* mutants. This notion was further supported by the observation that mutations in the *phyA* gene also largely suppressed the randomized-hypocotyl growth phenotype of *atmdr1-100* hypocotyls in far-red light. Thus, this work supports the proposition that AtMDR1 and regulated auxin transport act to promote hypocotyl elongation by repressing phyA-dependent far-red light signaling.

## MATERIALS AND METHODS

### Plant Materials and Growth Conditions

The T-DNA mutant *atmdr1-100* was isolated by screening a collection of activation-tagging T-DNA insertion lines ABRC CS21991 (Weigel et al., 2000). *atmdr1-101* (Salk_033455), *atmdr1-102* (Salk_031406), *atpgp1-100* (Salk_083649), and *atpgp1-101* (Salk_046440) were obtained from ABRC (Ohio State University, Columbus, OH). Their ecotype is Col. The *phyA-211* (Reed et al., 1994) and

*axr1-3* (Lincoln et al., 1990) mutants and the *DR5*::*GUS* reporter gene (Sabatini et al., 1999) are also derived from the Col background. The ecotype of *phyA-1* is L*er* (Whitelam et al., 1993). The insertion mutants have been backcrossed once or twice with their wild type to remove/reduce potential background mutations. The T-DNA insertion sites were confirmed by PCR and sequencing. Homozygous lines were selected by their phenotype and further verified by PCR genotyping.

Seeds were sterilized by incubation in freshly prepared 30% bleach plus 0.01% (v/v) Triton X-100 for 15 min and then washed four times with sterile water. The surface-sterilized seeds were sown on germination plates (1× Murashige and Skoog media supplied with 1% [w/v] Suc) and cold treated for 3 d at 4°C. After exposure to white light for 24 h to stimulate germination, plates with seeds were transferred to appropriate light conditions for 3 to 5 d at 22°C. Far-red, red, and blue lights were supplied by LED light sources, with irradiance fluence rates of approximately 0.5 $\mu$mol/m$^2$ s, 30 $\mu$mol/m$^2$ s, and 5 $\mu$mol/m$^2$ s, respectively, unless otherwise indicated (measured with International Light model IL1400A with sensor model SEL-033/F/W, Newburyport, MA). White light was supplied by cool-white fluorescent lamps.

## TAIL-PCR and PCR Genotyping

Genomic DNA was prepared with DNeasy Plant Mini kits (Qiagen USA, Valencia, CA). To obtain the flanking sequence of the C9-2 mutant, TAIL-PCR was carried out according to the method of Liu et al. (1995). The T-DNA left-border primers of pSKI015 vector were: TLB1 (5′-ACA CGT CGA AAT AAA GAT TTC CG-3′, for primary PCR), TLB2 (5′-TGC TTT CGC CTA TAA ATA CGA CG-3′, for secondary PCR), and TLB3 (5′-ATA ATA ACG CTG CGG ACA TCT AC-3′, for tertiary PCR). The PCR products were separated on 1% agarose gels, purified, and sequenced.

Due to the loss of antibiotic resistance in some T-DNA mutants, we used PCR genotyping to verify homozygous lines. PCR primers used for verifying the *atmdr1-100* allele were: TLB1, 28860-1 (5′-CGT TTA GCT ACT GAT GCA GC-3′) and 28860-2 (5′-CAG AAC CAT AGA GAG CAA GC-3′). PCR primers used for verifying the *atmdr1-101* mutant were: LB (5′-CGG AAC CAC CAT CAA ACA GG-3′, pROK2 T-DNA left-border primer), 28860-3 (5′-GAG AGT AAG GCA CTT AAT GC-3′), and 28860-4 (5′-CAA AAC TTG TTG CAT CAG GC-3′). PCR primers used for verifying the *atmdr1-102* mutant were: LB, 28860-1 and 28860-2.

To confirm the *atpgp1-100* and *atpgp1-101* alleles by PCR genotyping, primers LB, 36910-1 (5′-GGA GAG AGG ATT GCA GCT GT-3′) and 36910-2 (5′-GAC AAG GAC AAG TGC GAG TC-3′) were used.

## RT-PCR

Plant total RNA was extracted from rosette leaves using RNeasy Plant Mini kits (Qiagen USA). RT and PCR were conducted using the Access RT-PCR System following the manufacturer's instruction (Promega, Madison, WI). After RT at 48°C for 45 min, PCR was performed for a total of 25 cycles as follows: denaturation at 94°C for 30 s, annealing at 60°C for 1 min, and extension at 68°C for 1 min. The final extension was carried out at 68°C for 10 min. Primers used for RT-PCR were: Actin-F (5′-CAT CAG GAA GGA CTT GTA CGG-3′) and Actin-R (5′-GAT GGA CCT GAC TCG TCA TAC-3′) for *Actin* (*ACT1*) control, 28860-1 and 28860-2 for *AtMDR1*, 36910-1 and 36910-2 for *AtPGP1*.

## Construction of Double Mutant and Mutant Carrying DR5::GUS Reporter

The *atmdr1-100/phyA-1*, *atmdr1-100/atpgp1-100*, and *atmdr1-100/axr1-3* double mutants were derived from genetic crosses of their corresponding single-parental mutants. Putative double mutants were selected in $F_2$ generation and confirmed in F3 generation based on the mutant phenotype and PCR genotyping. The *DR5*::*GUS* reporter gene was introduced into *atmdr1-100* mutant by genetic crossing, and the homozygous lines were selected in $F_2$ generation and confirmed in F3 generation by PCR genotyping and GUS staining for the *atmdr1-100* mutation and the *DR5*::*GUS* reporter gene, respectively.

## Chlorophyll and Anthocyanin Measurement

Chlorophyll and anthocyanin measurement of seedlings was conducted according to Fankhauser and Casal (2004).

## Measurement of Hypocotyls Growth Orientation and Statistical Methods

Seedlings were vertically grown for 5 d, and the plates were photographed with a digital camera (Nikon Coolpix 4500, Tokyo). The angle measurement was taken by NIH Image software (developed at the United States National Institutes of Health and available on the Internet at http://rsb.info.nih.gov/nih-image). Statistical analysis was conducted as described (Robson and Smith, 1996).

## Hormone Treatment

For root elongation and lateral-root formation assays, seeds were placed on germination plates and grown vertically for 3 d under continuous white light or far-red light. The seedlings were then transferred to new plates (unsupplemented or supplemented with either 2,4-D, 1-NAA, or NPA). The positions of the primary root tips were marked. The seedlings were then grown vertically under continuous white light or far-red light for four more days, and the additional root growth was measured with a ruler. The percentage of relative root elongation was calculated based on control plants grown on unsupplemented media. Lateral roots were scored under a dissecting microscope, and a lateral root was accounted for if a visible primordium had formed.

For auxin transport assay, wild type (Col) and *atmdr1-100* mutant harboring *DR5*::*GUS* reporter gene were grown on germination plates for 4 d, and then IAA, 1-NAA or 2,4-D were applied to the hypocotyl-root junction or root tip for 3 h as described (Rashotte et al., 2000). For NPA treatment, seedlings were grown in germination plates for 3 d and then transferred to plates containing NPA for 24 h before GUS staining.

## Gravitropism Assay

Seedlings were grown vertically on square petri plates with or without 2.0 $\mu$M NPA in dark for 2 d, and then the plates were reorientated 90°. The angles of curvature were measured with a protractor every 6 h over a 24-h period as described (Rashotte et al., 2001). For GUS staining, seedlings were grown vertically on germination plates under white light for 4 d and then were transferred to new plates with (2.0 $\mu$M) or without NPA for 24 h. The plates were rotated 90°, and samples were subjected to GUS staining 3, 5, or 8 h after the gravistimulation.

## GUS Histochemical Assay

GUS staining was performed as previously described (Jefferson et al., 1987). Whole seedlings of wild type (Col) and *atmdr1-100* mutant harboring *DR5*::*GUS* reporter gene were harvested and incubated in 0.1 M sodium phosphate buffer containing 50 mM $K_3Fe(CN)_6$, 50 mM $K_4Fe(CN)_6$, and 1 mM 5-bromo-4-chloro-3-indolyl-$\beta$-D-glucuronide at 37°C for 3 h or overnight before examination under a microscope.

## Northern Blotting

Northern-blotting analysis was performed as previously described (Yang et al., 2005). An RT-PCR fragment of *AtMDR1* was used for probe labeling. Fragments of *RBCS*, *CAB3*, *CHS*, *PORA*, and *18S* rRNA used for labeling were described by Wang and Deng (2002) and Yang et al. (2005). The signals were quantified with a PhosphoImager (Storm 840, Molecular Dynamics, Sunnyvale, PA). The relative expressions were calculated by normalizing each signal against that of 18S rRNA.

## ACKNOWLEDGMENTS

We thank Georg Jander and Elizabeth Estabrook (Boyce Thompson Institute, Ithaca, NY) for their reading of and comments on the manuscript. We also thank Rujin Chen (Samuel Roberts Noble Foundation, Ardmore, OK) for helpful discussion during the course of this work. Thanks are also due to ABRC for distributing seeds.

Received February 17, 2005; revised March 17, 2005; accepted March 19, 2005; published May 20, 2005.

## LITERATURE CITED


**Alonso JM, Stepanova AN, Leisse TJ, Kim CJ, Chen H, Shinn P, Stevenson DK, Zimmerman J, Barajas P, Cheuk R, et al** (2003) Genome-wide insertional mutagenesis of *Arabidopsis thaliana*. Science **301:** 653–657

**Barnes SA, Nishizawa NK, Quaggio RB, Whitelam GC, Chua NH** (1996) Far-red light blocks greening of Arabidopsis seedlings via a phytochrome A-mediated change in plastid development. Plant Cell **8:** 601–615

**Behringer FJ, Davies PJ** (1992) Indole-3-acetic acid levels after phytochrome-mediated changes in the stem elongation rate of dark- and light-grown Pisum seedlings. Planta **188:** 85–92

**Buer CS, Muday GK** (2004) The *transparent testa4* mutation prevents flavonoid synthesis and alters auxin transport and the response of Arabidopsis roots to gravity and light. Plant Cell **16:** 1191–1205

**Casimiro I, Marchant A, Bhalerao RP, Beeckman T, Dhooge S, Swarup R, Graham N, Inze D, Sandberg G, Casero PJ, et al** (2001) Auxin transport promotes Arabidopsis lateral root initiation. Plant Cell **13:** 843–852

**Chen R, Hilson P, Sedbrook J, Rosen E, Caspar T, Masson PH** (1998) The *Arabidopsis thaliana AGRAVITROPIC 1* gene encodes a component of the polar-auxin-transport efflux carrier. Proc Natl Acad Sci USA **95:** 15112–15117

**Cluis CP, Mouchel CF, Hardtke CS** (2004) The Arabidopsis transcription factor HY5 integrates light and hormone signaling pathways. Plant J **38:** 332–347

**Colón-Carmona A, Chen DL, Yeh K-C, Abel S** (2000) Aux/IAA proteins are phosphorylated by phytochrome in vitro. Plant Physiol **124:** 1728–1738

**Dharmasiri N, Estelle M** (2004) Auxin signaling and regulated protein degradation. Trends Plant Sci **9:** 302–308

**Fankhauser C, Casal JJ** (2004) Phenotypic characterization of a photomorphogenic mutant. Plant J **39:** 747–760

**Friml J, Palme K** (2002) Polar auxin transport: old questions and new concepts? Plant Mol Biol **49:** 273–284

**Gaedeke N, Klein M, Kolukisaoglu U, Forestier C, Müller A, Ansorge M, Becker D, Mamnun Y, Kuchler K, Schulz B, et al** (2001) The *Arabidopsis thaliana* ABC transporter *A*tMRP5 controls root development and stomata movement. EMBO J **20:** 1875–1887

**Geisler M, Kolukisaoglu HU, Bouchard R, Billion K, Berger J, Saal B, Frangne N, Koncz-Kalman Z, Koncz C, Dudler R, et al** (2003) TWISTED DWARF1, a unique plasma membrane-anchored immunophilin-like protein, interacts with Arabidopsis multidrug resistance-like transporters AtPGP1 and AtPGP19. Mol Biol Cell **14:** 4238–4249

**Gil P, Dewey E, Friml J, Zhao Y, Snowden KC, Putterill J, Palme K, Estelle M, Chory J** (2001) BIG: a calossin-like protein required for polar auxin transport in Arabidopsis. Genes Dev **15:** 1985–1997

**Iino M** (1982) Inhibitory action of red light on growth of the maize mesocotyl: evaluation of the auxin hypothesis. Planta **156:** 388–395

**Jefferson RA, Kavanagh TA, Bevan MW** (1987) GUS fusions: beta-glucuronidase as a sensitive and versatile gene fusion marker in higher plants. EMBO J **6:** 3901–3907

**Jensen PJ, Hangarter RP, Estelle M** (1998) Auxin transport is required for hypocotyl elongation in light-grown but not dark-grown Arabidopsis. Plant Physiol **116:** 455–462

**Jones AM, Cochran D, Lamerson PM, Evans ML, Cohen JD** (1991) Red light-regulated growth: changes in the abundance of indolacetic acid and a 22-kilodalton auxin-binding protein in the maize mesocotyl. Plant Physiol **97:** 352–358

**Kim BC, Soh MS, Hong SH, Furuya M, Nam HG** (1998) Photomorphogenic development of the Arabidopsis *shy2-1D* mutation and its interaction with phytochromes in darkness. Plant J **15:** 61–68

**Klein M, Geisler M, Suh SJ, Kolukisaoglu HÜ, Azevedo L, Plaza S, Curtis MD, Richter A, Weder B, Schulz B, et al** (2004) Disruption of *AtMRP4,* a guard cell plasma membrane ABCC-type ABC transporter, leads to deregulation of stomatal opening and increased drought susceptibility. Plant J **39:** 219–236

**Klein M, Perfus-Barbeoch L, Frelet A, Gaedeke N, Reinhardt D, Mueller-Roeber B, Martinoia E, Forestier C** (2003) The plant multidrug resistance ABC transporter AtMRP5 is involved in guard cell hormonal signalling and water use. Plant J **33:** 119–129

**Kraepiel Y, Marrec K, Sotta B, Caboche M, Miginiac E** (1995) In vitro morphogenic characteristics of phytochrome mutants in *Nicotiana plumbaginifolia* are modified and correlated to high indole-3-acetic acid levels. Planta **197:** 142–146

**Leyser HM, Pickett FB, Dharmasiri S, Estelle M** (1996) Mutations in the *AXR3* gene of Arabidopsis result in altered auxin response including ectopic expression from the *SAUR-AC1* promoter. Plant J **10:** 403–413

**Lin C** (2002) Blue light receptors and signal transduction. Plant Cell **14:** S207–S225

**Lincoln C, Britton JH, Estelle M** (1990) Growth and development of *axr1* mutants of Arabidopsis. Plant Cell **2:** 1071–1080

**Liu YG, Mitsukawa N, Oosumi T, Whittier RF** (1995) Efficient isolation and mapping of *Arabidopsis thaliana* T-DNA insert junctions by thermal asymmetric interlaced PCR. Plant J **8:** 457–463

**Ma L, Li J, Qu L, Hager J, Chen Z, Zhao H, Deng XW** (2001) Light control of Arabidopsis development entails coordinated regulation of genome expression and cellular pathways. Plant Cell **13:** 2589–2607

**Marchant A, Kargul J, May ST, Muller P, Delbarre A, Perrot-Rechenmann C, Bennett MJ** (1999) AUX1 regulates root gravitropism in Arabidopsis by facilitating auxin uptake within root apical tissues. EMBO J **18:** 2066–2073

**Martinoia E, Klein M, Geisler M, Bovet L, Forestier C, Kolukisaoglu U, Muller-Rober B, Schulz B** (2002) Multifunctionality of plant ABC transporters: more than just detoxifiers. Planta **214:** 345–355

**McNellis TW, Deng XW** (1995) Light control of seedling morphogenetic pattern. Plant Cell **7:** 1749–1761

**Møller SG, Kunkel T, Chua NH** (2001) A plastidic ABC protein involved in intercompartmental communication of light signaling. Genes Dev **15:** 90–103

**Muday GK, Murphy AS** (2002) An emerging model of auxin transport regulation. Plant Cell **14:** 293–299

**Müller A, Guan C, Gälweiler L, Tanzler P, Huijser P, Marchant A, Parry G, Bennett M, Wisman E, Palme K** (1998) *AtPIN2* defines a locus of Arabidopsis for root gravitropism control. EMBO J **17:** 6903–6911

**Multani DS, Briggs SP, Chamberlin MA, Blakeslee JJ, Murphy AS, Johal GS** (2003) Loss of an MDR transporter in compact stalks of maize *br2* and sorghum *dw3* mutants. Science **302:** 81–84

**Murphy AS, Hoogner KR, Peer WA, Taiz L** (2002) Identification, purification, and molecular cloning of n-1-naphthylphthalmic acid-binding plasma membrane-associated aminopeptidases from Arabidopsis. Plant Physiol **128:** 935–950

**Nagpal P, Walker LM, Young JC, Sonawala A, Timpte C, Estelle M, Reed JW** (2000) *AXR2* encodes a member of the Aux/IAA protein family. Plant Physiol **123:** 563–573

**Neff MM, Fankhauser C, Chory J** (2000) Light: an indicator of time and place. Genes Dev **14:** 257–271

**Nemhauser JL, Chory J** (2002) Photomorphogenesis. *In* CR Somerville, E Meyerowitz, eds, The Arabidopsis Book. American Society of Plant Biologists, Rockville, MD, http://www.bioone.org/pdfserv/i1543-8120-008-01-0001.pdf

**Noh B, Bandyopadhyay A, Peer WA, Spalding EP, Murphy AS** (2003) Enhanced gravi- and phototropism in plant *mdr* mutants mislocalizing the auxin efflux protein PIN1. Nature **423:** 999–1002

**Noh B, Murphy AS, Spalding EP** (2001) Multidrug resistance-like genes of Arabidopsis required for auxin transport and auxin-mediated development. Plant Cell **13:** 2441–2454

**Ottenschläger I, Wolff P, Wolverton C, Bhalerao RP, Sandberg G, Ishikawa H, Evans M, Palme K** (2003) Gravity-regulated differential auxin transport from columella to lateral root cap cells. Proc Natl Acad Sci USA **100:** 2987–2991

**Quail PH** (2002) Photosensory perception and signalling in plant cells: new paradigms? Curr Opin Cell Biol **14:** 180–188

**Rashotte AM, Brady SR, Reed RC, Ante SJ, Muday GK** (2000) Basipetal auxin transport is required for gravitropism in roots of Arabidopsis. Plant Physiol **122:** 481–490

**Rashotte AM, Delong A, Muday GK** (2001) Genetic and chemical reductions in protein phosphatase activity alter auxin transport, gravity response, and lateral root growth. Plant Cell **13:** 1683–1697

**Reed JW, Nagatani A, Elich TD, Fagan M, Chory J** (1994) Phytochrome A and phytochrome B have overlapping but distinct functions in Arabidopsis development. Plant Physiol **104:** 1139–1149

**Robson PRH, Smith H** (1996) Genetic and transgenic evidence that phytochromes A and B act to modulate the gravitropic orientation of *Arabidopsis thaliana* hypocotyls. Plant Physiol **110:** 211–216

**Romano CP, Robson PRH, Smith H, Estelle M, Klee H** (1995) Transgene–mediated auxin overproduction in Arabidopsis: hypocotyl elongation phenotype and interaction with the *hy6-1* hypocotyl elongation and *axr1* auxin-resistant mutants. Plant Mol Biol **27:** 1071–1083

**Ruegger M, Dewey E, Hobbie L, Brown D, Bernasconi P, Turner J, Muday G, Estelle M** (1997) Reduced naphthylphthalamic acid binding in the *tir3* mutant of Arabidopsis is associated with a reduction in polar auxin transport and diverse morphological defects. Plant Cell **9:** 745–757

**Sabatini S, Beis D, Wolkenfelt H, Murfett J, Guilfoyle T, Malamy J, Benfey P, Leyser O, Bechtold N, Weisbeek P, et al** (1999) An auxin-dependent distal organizer of pattern and polarity in the Arabidopsis root. Cell **99:** 463–472

**Sánchez-Fernández R, Davies TG, Coleman JO, Rea PA** (2001) The *Arabidopsis thaliana* ABC protein superfamily: a complete inventory. J Biol Chem **276:** 30231–30244

**Schwechheimer C, Serino G, Callis J, Crosby WL, Lyapina S, Deshaies RJ, Gray WM, Estelle M, Deng XW** (2001) Interactions of the COP9 signalosome with the E3 ubiquitin ligase $SCF^{TIR1}$ in mediating auxin response. Science **292:** 1379–1382

**Shinkle JR, Kadakia R, Jones AM** (1998) Dim-red-light-induced increase in polar auxin transport in cucumber seedlings: development of altered capacity, velocity, and response to inhibitors. Plant Physiol **116:** 1505–1513

**Sidler M, Hassa P, Hasan S, Ringli C, Dudler R** (1998) Involvement of an ABC transporter in a developmental pathway regulating hypocotyl cell elongation in the light. Plant Cell **10:** 1623–1636

**Steindler C, Matteucci A, Sessa G, Weimar T, Ohgishi M, Aoyama T, Morelli G, Ruberti I** (1999) Shade avoidance responses are mediated by the ATHB-2 HD-Zip protein, a negative regulator of gene expression. Development **126:** 4235–4245

**Swarup R, Parry G, Graham N, Allen T, Bennett M** (2002) Auxin cross-talk: integration of signaling pathways to control plant development. Plant Mol Biol **49:** 411–426

**Tian Q, Reed JW** (1999) Control of auxin-regulated root development by the *Arabidopsis thaliana SHY2/IAA3*. Development **126:** 711–721

**Tian Q, Reed JW** (2001) Molecular links between light and auxin signaling pathways. J Plant Growth Regul **20:** 274–280

**Walton JD, Ray PM** (1981) Evidence for receptor function of auxin binding sites in maize: red light inhibition of mesocotyl elongation and auxin binding. Plant Physiol **68:** 1334–1338

**Wang H, Deng XW** (2002) Arabidopsis FHY3 defines a key phytochrome A signaling component directly interacting with its homologous partner FAR1. EMBO J **21:** 1339–1349

**Wang H, Deng XW** (2004) Phytochrome signaling mechanism. *In* CR Somerville, E Meyerowitz, eds, The Arabidopsis Book. American Society of Plant Biologists, Rockville, MD. http://www.bioone.org/pdfserv/i1543-8120-018-01-0001.pdf

**Weigel D, Ahn JH, Blázquez MA, Borevitz JO, Christensen SK, Fankhauser C, Ferrándiz C, Kardailsky I, Malancharuvil EJ, Neff MM, et al** (2000) Activation tagging in Arabidopsis. Plant Physiol **122:** 1003–1014

**Whitelam GC, Johnson E, Peng J, Carol P, Anderson ML, Cowl JS, Harberd NP** (1993) Phytochrome A null mutants of Arabidopsis display a wild-type phenotype in white light. Plant Cell **5:** 757–768

**Windsor B, Roux SJ, Lloyd A** (2003) Multiherbicide tolerance conferred by AtPGP1 and apyrase overexpression in *Arabidopsis thaliana*. Nat Biotechnol **21:** 428–433

**Yang J, Lin R, Sullivan J, Hoecker U, Liu B, Xu L, Deng XW, Wang H** (2005) Light regulates COP1-mediated degradation of HFR1, a transcription factor essential for light signaling in Arabidopsis. Plant Cell **17:** 804–821

**Zhao Y, Christensen SK, Fankhauser C, Cashman JR, Cohen JD, Weigel D, Chory J** (2001) A role for flavin monooxygenase-like enzymes in auxin biosynthesis. Science **291:** 306–309